

Atomic structure and electronic properties of hydrogenated X (=C, Si, Ge, and Sn) doped TiO₂ : A theoretical perspective

Filippatos, P. P., Kelaidis, N., Vasilopoulou, M., Davazoglou, D. & Chroneos, A.

Published PDF deposited in Coventry University's Repository

Original citation:

Filippatos, PP, Kelaidis, N, Vasilopoulou, M, Davazoglou, D & Chroneos, A 2020, 'Atomic structure and electronic properties of hydrogenated X (=C, Si, Ge, and Sn) doped TiO₂ : A theoretical perspective', AIP Advances, vol. 10, 115316, pp. 115316-1 to 115316-11.

<https://dx.doi.org/10.1063/5.0032564>

DOI 10.1063/5.0032564

ESSN 2158-3226

Publisher: American Institute of Physics

© 2020 Author(s). All article content, except where otherwise noted, is licensed under a Creative Commons Attribution (CC BY) license (<http://creativecommons.org/licenses/by/4.0/>).

Copyright © and Moral Rights are retained by the author(s) and/ or other copyright owners. A copy can be downloaded for personal non-commercial research or study, without prior permission or charge. This item cannot be reproduced or quoted extensively from without first obtaining permission in writing from the copyright holder(s). The content must not be changed in any way or sold commercially in any format or medium without the formal permission of the copyright holders.

Atomic structure and electronic properties of hydrogenated X (=C, Si, Ge, and Sn) doped TiO₂: A theoretical perspective

Cite as: AIP Advances **10**, 115316 (2020); <https://doi.org/10.1063/5.0032564>

Submitted: 09 October 2020 . Accepted: 29 October 2020 . Published Online: 13 November 2020

Petros-Panagis Filippatos,  Nikolaos Kelaidis, Maria Vasilopoulou, Dimitris Davazoglou, and  Alexander Chroneos

COLLECTIONS

Paper published as part of the special topic on [Chemical Physics](#), [Energy, Fluids and Plasmas](#), [Materials Science](#) and [Mathematical Physics](#)



View Online



Export Citation



CrossMark

ARTICLES YOU MAY BE INTERESTED IN

[A perspective on MXenes: Their synthesis, properties, and recent applications](#)

Journal of Applied Physics **128**, 170902 (2020); <https://doi.org/10.1063/5.0021485>

[Deep level transient spectroscopy investigation of ultra-wide bandgap \(201\) and \(001\) \$\beta\$ -Ga₂O₃](#)

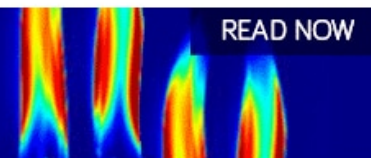
Journal of Applied Physics **128**, 205701 (2020); <https://doi.org/10.1063/5.0021859>

[First-principles study of point defects in LiGaO₂](#)

Journal of Applied Physics **126**, 155703 (2019); <https://doi.org/10.1063/1.5126028>

AIP Advances
Fluids and Plasmas Collection

READ NOW



Atomic structure and electronic properties of hydrogenated X (=C, Si, Ge, and Sn) doped TiO₂: A theoretical perspective

Cite as: AIP Advances 10, 115316 (2020); doi: 10.1063/5.0032564

Submitted: 9 October 2020 • Accepted: 29 October 2020 •

Published Online: 13 November 2020



Petros-Panagis Filippatos,^{1,2} Nikolaos Kelaidis,^{2,3}  Maria Vasilopoulou,¹ Dimitris Davazoglou,¹ and Alexander Chrones^{2,4,a)} 

AFFILIATIONS

¹Institute of Nanoscience and Nanotechnology (INN), National Center for Scientific Research Demokritos, 15310 Agia Paraskevi, Athens, Greece

²Faculty of Engineering, Environment and Computing, Coventry University, Priory Street, Coventry CV1 5FB, United Kingdom

³Theoretical and Physical Chemistry Institute, National Hellenic Research Foundation, Vass. Constantinou 48, GR-11635 Athens, Greece

⁴Department of Materials, Imperial College, London SW7 2AZ, United Kingdom

^{a)}Author to whom correspondence should be addressed: ab8104@coventry.ac.uk

ABSTRACT

Titanium dioxide (TiO₂) and especially its polymorph, anatase, are widely used transition-metal oxides for renewable energy applications such as photocatalytic and photovoltaic devices due to their chemical stability and their electrochemical and photocatalytic properties. However, the wide energy bandgap of anatase limits its photocatalytic ability and electron transport properties. Doping with appropriate elements is an established way to control and tune the optical and electronic properties of anatase such as conductivity, transparency, and bandgap. Metal doping can improve anatase's properties as an electron transport layer, whereas non-metal (anion) doping is widely used to improve its photocatalytic activity. Herein, we investigate the effect of carbon group dopants in conjunction with hydrogenation of TiO₂ by applying density functional theory. We find that hydrogenation has a positive impact on the structural and electronic properties of TiO₂, thus making it an appropriate candidate for energy harvesting devices.

© 2020 Author(s). All article content, except where otherwise noted, is licensed under a Creative Commons Attribution (CC BY) license (<http://creativecommons.org/licenses/by/4.0/>). <https://doi.org/10.1063/5.0032564>

I. INTRODUCTION

Following the systematic study of Fujishima and Honda,¹ TiO₂ and many other metal oxides, such as tin oxide (SnO₂), tungsten trioxide (WO₃), and aluminum trioxide (Al₂O₃), have been extensively investigated due to their interesting photocatalytic properties, high chemical stability, and long lifetime photo-generated carriers.^{1–10} Anatase TiO₂ is often used as an electron transport material in organic solar cells (OSCs) and perovskite solar cells (PSCs) due to its intrinsic *n*-type conductivity and adequate electron mobility attributed to oxygen vacancies formed during deposition. However, anatase has a wide bandgap (3.2 eV) that limits its absorption in visible-light and near-infrared (NIR) regions.¹¹ To increase the catalytic performance of anatase TiO₂, many strategies have been

investigated, such as formulation of ternary oxides,^{12,13} defect engineering (e.g., halogen doping¹⁴ and formation of oxygen vacancies), application of stresses,¹⁵ and introduction of disorder in the lattice.¹⁶ In this context, Chen *et al.*¹⁶ engineered anatase TiO₂ and, through hydrogen doping, synthesized the so-called black titania with a bandgap of 1.54 eV due to an upward shifted valence band (VB) edge by hydrogen insertion. The hydrogen concentration of their samples was 0.25 wt. %, which corresponds to one H atom per five Ti atoms. Their results point to a strong dependence of the electronic properties on the hydrogen concentration. Through density functional theory (DFT) calculations, Liu *et al.*¹⁷ predicted that hydrogen atoms contribute to surface disordering, by breaking Ti–O bonds and creating Ti–H and H–O pairs.¹⁷ Other studies suggested that the improvement in the visible-light

absorption is related to the formation of the bonds on the surface of H:TiO_2 .^{18–21}

Besides hydrogen, many transition-metal cations have been also used as dopants in TiO_2 .^{22–25} However, it is expected that despite the conductivity enhancement upon doping, the enhanced photocatalytic activity of cation-doped TiO_2 might be because the dopant-related localized d-states act as recombination centers for the photogenerated carriers.^{22–25} Conversely, carbon dopants amplify the photocatalytic activity of TiO_2 in the visible-light region as they introduce new states inside the bandgap without acting as recombination centers.^{26–29} Doping with both C and N results in about a 50 nm red shift in the absorption spectra^{26–29} and produces photoactivity in the visible-light region. Recent results with carbon doping further demonstrate improved photocatalytic efficiency in water splitting with a total conversion efficiency of up to 11%. Gao *et al.*³⁰ reported that doping of TiO_2 with carbon cations present in different oxidation states influences the crystal structure, the charge density, and the optical properties compared to the pure TiO_2 . However, in the literature, there are many explanations for the enhanced photocatalytic activity of C:TiO_2 .^{30–34}

For silicon doping of TiO_2 (Si:TiO_2), Oh *et al.*³⁵ predicted that in small dopant concentrations, Si could improve the photocatalytic properties of TiO_2 . Yan *et al.*³⁶ indicated that the substitutional doping of Ti with Si causes a broadening of the optical absorption. Moreover, Ozaki *et al.*³⁷ prepared N:Si:TiO_2 with strong absorption in the visible-light region and with high photocatalytic activity. Other dopants, such as germanium (Ge), can also reduce the bandgap of TiO_2 , whereas tin (Sn) doping of TiO_2 causes a slight bandgap broadening.³⁸ From an experimental point of view, Li and Zeng³⁹ showed that in the case of Sn:TiO_2 , the bandgap is reduced about 0.13 eV when Sn is inserted as a substitution for Ti in a small concentration. Xiong and Balkus⁴⁰ also predicted that the photodegradation of various dyes for Sn:TiO_2 is more effective than for P25 and the pure TiO_2 . To sum up, both H:TiO_2 and $\text{X}(=\text{C, Si, Ge, Sn})$ doping of TiO_2 show improvement in the photocatalytic and electronic properties. So, it would be interesting to investigate whether and how co-doping can act synergistically and further benefit the optical properties.

In the present study, we apply DFT computational methods to investigate the effect of doping anatase TiO_2 with C, Si, Ge, and Sn in conjunction with H. Therefore, we examine the effect of each dopant on the hydrogenated TiO_2 and compare it with non-hydrogenated TiO_2 . We look into the possible binding of the dopant $\text{X}(=\text{C, Si, Ge, and Sn})$ with H and cluster formation. Finally, we consider the density of states (DOS) of the minimum energy systems to assess the impact of doping and co-doping on the electronic properties of TiO_2 .

II. METHODOLOGY

For the DFT calculations, the plane wave code CASTEP^{41,42} was used, with exchange–correlation interactions modeled with the Perdew–Burke–Ernzerhof (PBE)⁴³ density functional in the generalized gradient approximation (GGA) with ultrasoft pseudopotentials.⁴⁴ The cut-off energy of the wave basis was set at 480 eV, in conjunction with a $2 \times 2 \times 3$ k-point Monkhorst–Pack⁴⁵ grid. For our calculations, a $3 \times 3 \times 1$ repeat unit cell, which results in a

108-atomic site supercell, was used. To include the effect of localized electrons, onsite Coulomb repulsions⁴⁶ of 8.2 eV were set for the 3d orbitals of Ti.¹⁵ The calculations were under constant pressure conditions. For the DOS calculations, a denser mesh of $3 \times 3 \times 3$ k-points was applied, whereas for the partial density of states (PDOS), the optados code was used with a denser mesh of $5 \times 5 \times 5$ k-points. The convergence criteria for the plain TiO_2 were calculated as follows: The spectral correction factor (SCF) tolerance was set at $2.0 \cdot 10^{-5}$ eV/atom, the maximum force tolerance was calculated as 0.05 eV/Å, the maximum stress tolerance was at 0.1 GPa, and the maximum displacement tolerance was at 0.001 Å. The efficacy of this approach was discussed in the previous work.^{14,15,47,48} Related techniques can provide significant insights into the electronic structure and defect engineering strategies that can improve energy materials.^{49–52}

III. RESULTS AND DISCUSSION

A. Structural properties

Anatase belongs to the tetragonal space group $I4/amd$ with lattice parameters $a = 3.782$ Å and $c = 9.502$ Å.⁵³ We calculate the lattice parameters of the perfect cell to be $a = 3.806$ Å and $c = 9.73$ Å for the unit cell and $a = 11.41$ Å, $c = 9.73$ Å, and volume = 1267.40 Å³ for the $3 \times 3 \times 1$ supercell. In order to examine the effect of doping on the anatase structure, we use the supercell method with a supercell of 108 atoms. The dopants (C, Si, Ge, and Sn) are examined in the Ti-substitutional position, which is more favorable energetically than the interstitial one, whereas hydrogen has been examined both as an interstitial dopant and as a substitutional dopant at O positions.

For each dopant X, we calculate the optimized geometry of the supercell with X as a substitutional dopant and then we study the effect of H on this structure, with H examined at an interstitial position or at a substitutional neighboring O position.

In this mode, for the C dopant, we examine the geometry of the cell at a (a) Ti substitutional position of non-hydrogenated anatase: $\text{C}_{\text{Ti}}:\text{TiO}_2$, (b) hydrogenated anatase with H at an interstitial position, $\text{H}_i:\text{C}_{\text{Ti}}:\text{TiO}_2$, and (c) $\text{H}_\text{O}:\text{C}_{\text{Ti}}:\text{TiO}_2$, hydrogenated anatase with H at a neighboring O substitution position. In Fig. 1, we present the calculated structures, whereas their structural parameters are shown in Table I.

Substitution of Ti for C produces a minimal distortion in the lattice. The C–O distance is 2.32 Å, which is larger than the standard Ti–O distance of 1.94 Å. It is therefore concluded that carbon increases the lattice constants and the cell volume, despite its smaller ionic radius compared to Ti^{4+} , which is in agreement with experimental results. Chen *et al.*⁵⁴ performed experiments on C:TiO_2 and, based on Bragg's law, calculated that the doping of TiO_2 with carbon slightly increases the lattice constants and the cell volume. The experimental results are presented in Table I for reference. We also calculated the relaxed system of minimum energy, where hydrogen is an interstitial defect (H_i). The preferred position of H at the lattice is calculated at a distance of 2.07 Å near the carbon atom. After H_i co-doping, the calculated lattice volume slightly decreases compared to that in carbon doping only, but it remains larger than of pristine TiO_2 . To explain the small decrease in lattice volume of $\text{C}_{\text{Ti}}:\text{TiO}_2$, we should take into account that as H_i binds to O, it makes it less electronegative, and as a result, the Ti–O

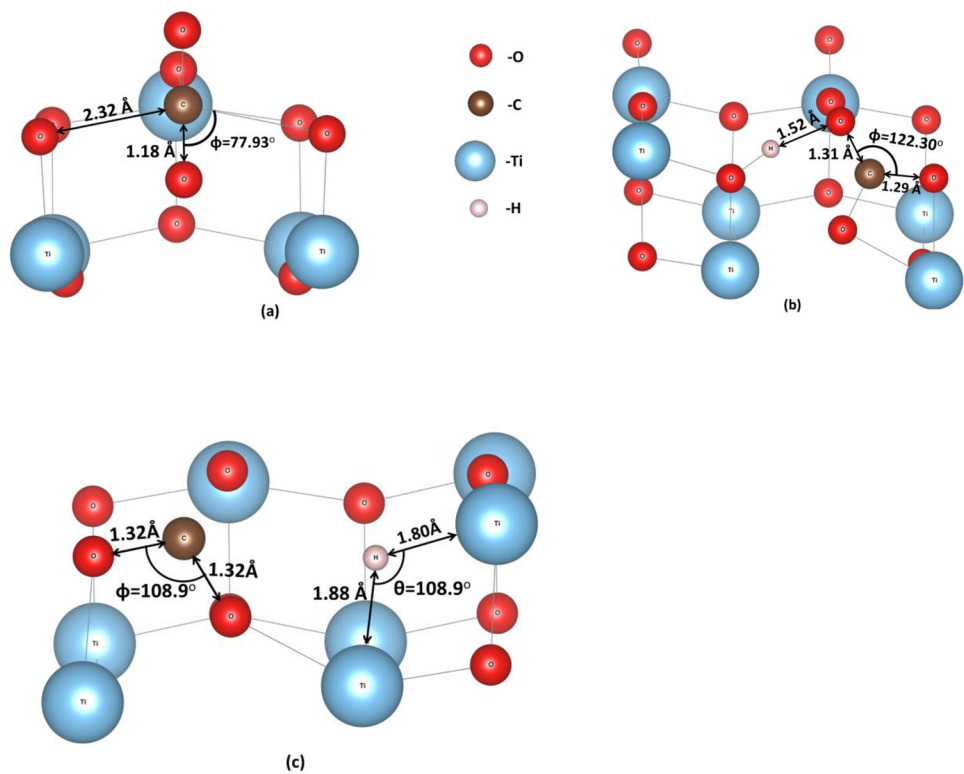


FIG. 1. Minimum energy structures in anatase: (a) C-Ti, (b) H-C-Ti, and (c) H-O-C-Ti.

bond becomes less ionic, with smaller electron density residing on Ti compared to the non-hydrogenated oxide. This leads to a weaker Ti-Ti repulsion, which decreases the Ti-Ti bond length, hence suppressing the lattice volume after hydrogen insertion at interstitial positions.

For the H₀:C_{Ti}:TiO₂ case, we predicted a reduction of the cell volume compared to that of C_{Ti}:TiO₂, but still, it was calculated

TABLE I. Lattice parameters and cell volumes for all the examined cases.

	a (Å)	b (Å)	c (Å)	Volume (Å ³)
TiO ₂	3.80	3.80	9.73	140.80
C _{Ti} :TiO ₂	3.84	3.84	9.66	142.84
H _i :C _{Ti} :TiO ₂	3.85	3.83	9.64	142.40
H ₀ :C _{Ti} :TiO ₂	3.84	3.81	9.61	141.12
Si _{Ti} :TiO ₂	3.79	3.79	9.71	139.89
H _i :Si _{Ti} :TiO ₂	3.80	3.81	9.68	140.27
H ₀ :Si _{Ti} :TiO ₂	3.79	3.81	9.68	140.18
Ge _{Ti} :TiO ₂	3.79	3.80	9.74	140.68
H _i :Ge _{Ti} :TiO ₂	3.81	3.81	9.71	141.15
H ₀ :Ge _{Ti} :TiO ₂	3.81	3.80	9.73	140.98
Sn _{Ti} :TiO ₂	3.81	3.81	9.77	141.73
H _i :Sn _{Ti} :TiO ₂	3.81	3.82	9.75	142.19
H ₀ :Sn _{Ti} :TiO ₂	3.82	3.80	9.76	141.80

larger than the TiO₂ volume. This reduction is explained on the basis of a smaller electron density residing on the Ti atoms upon oxygen substitution with hydrogen causing a weaker Ti-Ti repulsion and decrease in the bond length between Ti cations similarly to the previous explanation. Generally, in the examined H, C co-doped systems, the optimized structures become orthorhombic ($a > b$), in which the cell parameters a and b are larger, while c is slightly smaller than that of anatase TiO₂. The above result is in good agreement with other theoretical investigations.⁵⁵

Focusing on Fig. 2, the Si-doped case is presented. In Fig. 2(a), it is seen that Si can substitute a Ti atom. The supercell parameters and volume are significantly reduced. This can be attributed to the smaller ionic radius of Si⁴⁺ (40 pm) compared to Ti⁴⁺ (61 pm). After H_i and H₀ doping, the lattice constants were slightly increased, but again, they are smaller than those of the pure TiO₂. Similar works on Si:TiO₂ have also predicted a lattice volume reduction upon Si doping.^{56,57}

The H:Ge:TiO₂ case is presented in Fig. 3. First, it is calculated that Ge_{Ti} doping does not affect the lattice constants and the volume. This is because the ionic radius of Ge⁴⁺ (53 pm) is relatively close to that of Ti⁴⁺. Our results agree with the results of experiments performed by Chatterjee and Chatterjee.⁵⁸ Specifically, it was predicted that the lattice constant along the c axis decreases with the increase in the germanium concentration, while the a constant is seen to remain the same. After H_i and H₀ incorporation, the lattice constants and the volume are slightly increased.

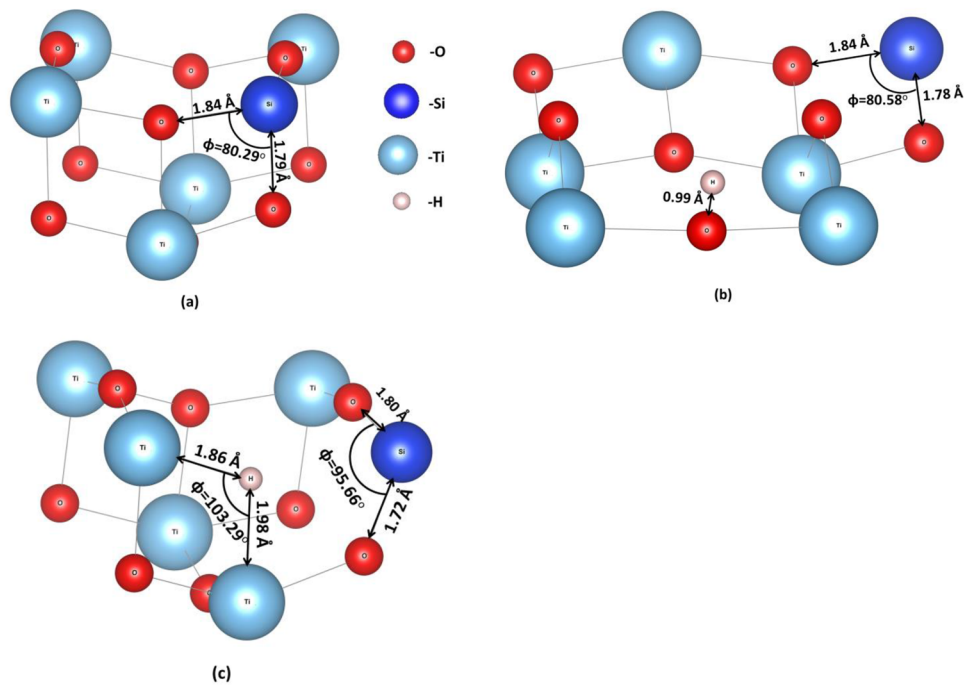


FIG. 2. Minimum energy structures in anatase: (a) Si-Ti , (b) $\text{H}_1\text{-Si-TiO}_2$, and (c) $\text{H}_2\text{-Si-TiO}_2$.

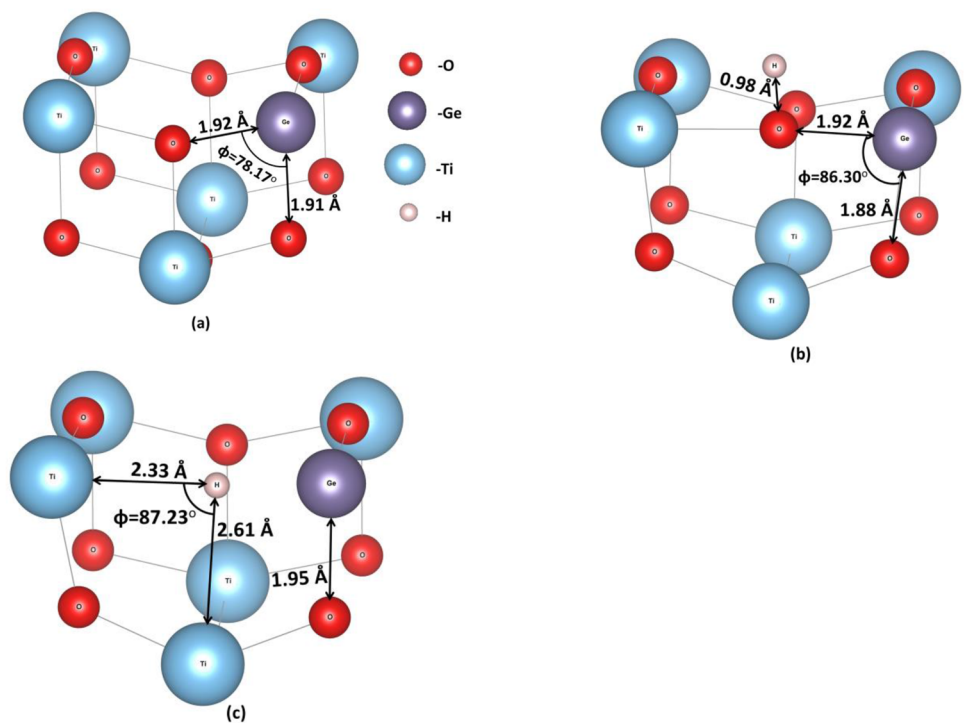


FIG. 3. Minimum energy structures in anatase: (a) Ge-Ti , (b) $\text{H}_1\text{-Ge-TiO}_2$, and (c) $\text{H}_2\text{-Ge-TiO}_2$. The germanium atom is in silver color, while hydrogen is in pink color.

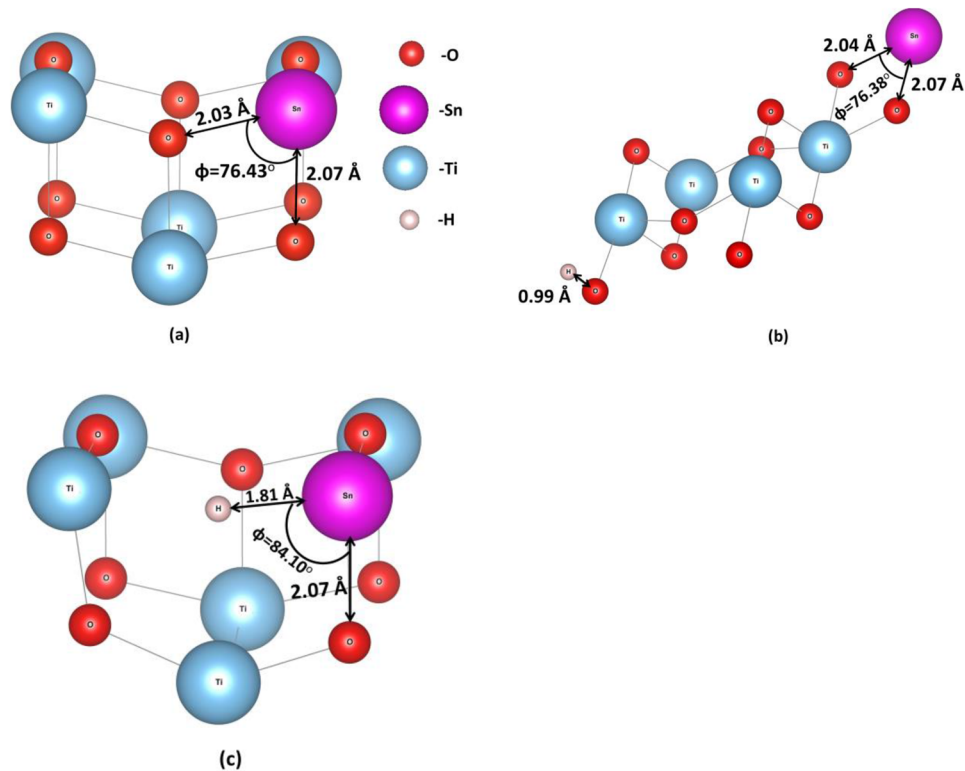


FIG. 4. Minimum energy structures in anatase: (a) Ge-Ti , (b) $\text{H}_i\text{-Ge-Ti}$, and (c) $\text{H}_o\text{-Ge-Ti}$. The tin atom is in orchid color, while hydrogen is in pink color.

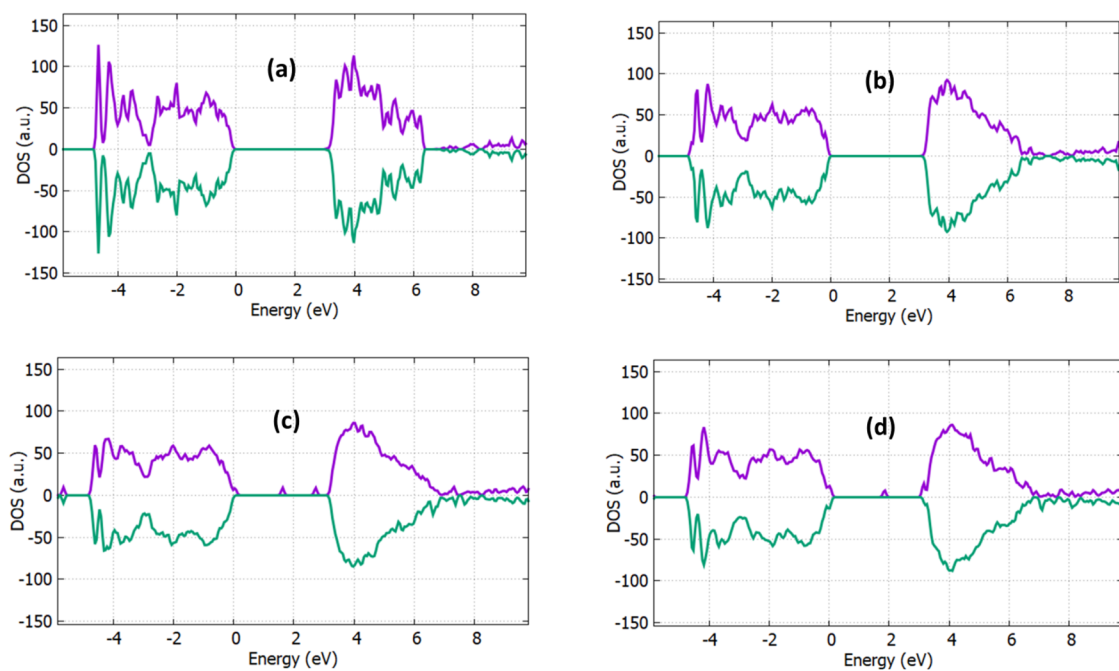


FIG. 5. Densities of states for (a) pure, (b) C_{Ti} doped, (c) H_i and C_{Ti} doped, and (d) H_o and C_{Ti} doped TiO_2 .

TABLE II. Bandgap values for the $X(\text{C, Si, Ge, Sn})$ -doped TiO_2 .

Dopant	TiO_2 (eV)	$\text{H}_i\text{:TiO}_2$ (eV)	$\text{H}_o\text{:TiO}_2$ (eV)
C	2.95	2.79	2.85
Si	2.90	2.85	2.70
Ge	2.98	2.80	2.85
Sn	3.0	2.75	2.88

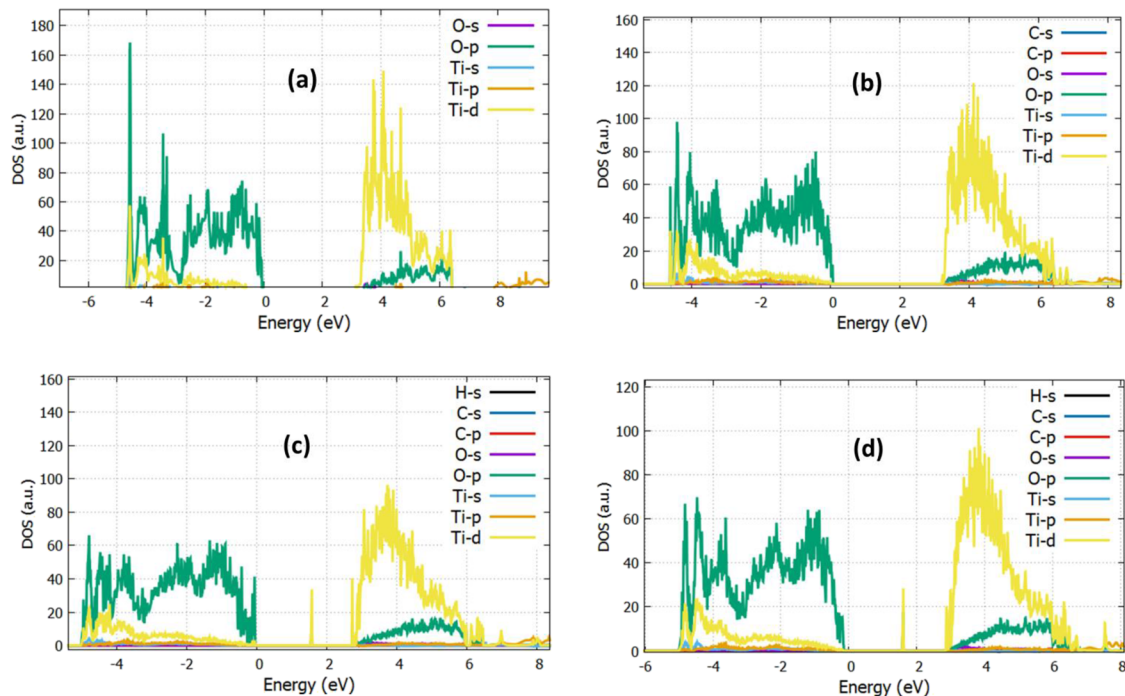
Last, we examined H:Sn:TiO_2 (Fig. 4). We predicted that the lattice constants and the volume of $\text{Sn}_{\text{Ti}}\text{:TiO}_2$ do not change significantly despite the larger ionic radius of Sn^{4+} (71 pm) compared to Ti^{4+} . In their experimental investigation, Duan *et al.*⁵⁹ also concluded that the anatase crystal structure is not significantly influenced by Sn doping. However, the dopant concentration was found to play an important role in varying the lattice constants. Again, in this case, hydrogen doping slightly increases the lattice constants. All the above structural results are presented in Table I. It is seen that only in the Si:TiO_2 and H:Si:TiO_2 cases, the supercell is reduced.

B. Electronic properties

The total density of states of the energetically minimum sites of the defects is considered in order for the electrical properties to be investigated. The present calculations were performed with the Hubbard +U model with $U = 8.2$ eV.^{14,15} The calculated bandgap

was 3.14 eV, in excellent agreement with the experimental value (3.2 eV). We present the total DOS of the pure TiO_2 in Fig. 5(a) for reference, and in Table II, we include the bandgap values for the doped TiO_2 . As we show in Fig. 5(b), $\text{C}_{\text{Ti}}\text{:TiO}_2$ has a DOS very similar in shape to that of the pure TiO_2 . It is seen that with substitutional carbon doping, the bandgap is calculated as 2.95 eV, in good agreement with other theoretical predictions.¹⁵ From an experimental point of view,⁵⁴ it is seen that the bandgap of C:TiO_2 reaches a value of 2.97 eV, which is in good agreement with our results. Focusing on the optical properties of C:TiO_2 , the UV-Vis experiments⁵⁴ showed that a noticeable shift of the absorption edge to the visible-light region is observed and this can be attributed to the predicted bandgap reduction. For the hydrogenated structure having additional interstitial H_i , the bandgap is further reduced to 2.80 eV [Fig. 5(c)], while with H as O-substitutional, the bandgap reaches a value of 2.85 eV [Fig. 5(d)]. In Fig. 6, the pDOS is presented. In Fig. 6(b), it is seen that the valence band is mainly created from the O-2p states, whereas the conduction band is created from Ti-3d.

When H is in the interstitial position, the calculations predict the creation of the gap states near the mid-gap and near the conduction band. The latter are very close to the conduction band minimum, hence constituting actor states for the co-doped oxide. In Fig. 6(c), it is seen that the gap states are created from hybridization of Ti-3d with O-2p and H-2s. In the case of $\text{H}_o\text{:C}_{\text{Ti}}\text{:TiO}_2$, again, mid-gap states are created. This implies that $\text{H}_i\text{:C}_{\text{Ti}}\text{:TiO}_2$ behaves as an electron acceptor, which is very important for its function as either a photocatalyst or an electron transport material, as these states are created near the valence band [Fig. 6(d)].

**FIG. 6.** Projected densities of states for (a) pure, (b) C_{Ti} doped, (c) H_i and C_{Ti} doped, and (d) H_o and C_{Ti} doped TiO_2 .

These states are created due to the hybridization of C-2p states with H-1s states as was described in the literature.⁵⁵ Notably, the mixing of O-2p states that mainly contribute to the VB with C-2p orbitals leads to an upward shift of the VB edge, hence resulting in the bandgap reduction. This reduction indicates that the photocatalytic ability of C:TiO₂ in the visible-light region might be due to the contribution of C-2p states to the VB maximum, while for the co-doped case, a higher photocatalytic activity is expected due to further bandgap narrowing upon the insertion of H within the crystal.

When TiO₂ is doped with Si_{Ti}, the bandgap is reduced to 2.90 eV, and this type of doping also creates some available states near the conduction band [Fig. 7(a)]. This result is in good agreement with that of the theoretical investigation of Lin *et al.*⁶¹ who calculated a bandgap of 2.9 eV. The experiments regarding Si:TiO₂⁵⁶ predicted a significant reduction of the bandgap of nearly 0.32 eV upon silicon incorporation, which is in close agreement with the reduction predicted herein. From the pDOS in Fig. 8(a), it is seen that the silicon 3p states mainly contribute to the valence band. When we dope Si_{Ti}:TiO₂ with H_i, we calculated that the bandgap is slightly reduced to 2.85 eV, with mid-gap states appearing at 1.95 eV. From the PDOS in Fig. 8(b), it is seen that these states are mainly attributed to the hybridization of Ti-3d with O-2p and H-2s orbitals. On the other hand, when hydrogen is an O-substitutional dopant, the bandgap is further reduced to 2.70 eV [Figs. 7(b) and 8(b)]. In this case, mid-gap states are calculated at 1.70 eV and available gap states at 2.72 eV. From all the above, it is expected that H_O:Si_{Ti}:TiO₂ also behaves as an acceptor (*n*-type semiconductor).

Continuing with the Ge_{Ti}:TiO₂ case, it is shown in Figs. 9(a) and 10(a) that the bandgap is reduced to 2.98 eV with Ge atoms

contributing to the valance band. This is in good agreement with the study of Chang *et al.*⁶² who calculated a bandgap of ~3 eV. The optical bandgap of Ge:TiO₂ was computed from UV-Vis experiments as 3 eV,⁵⁸ which is again in good agreement with our results. It was predicted that the substitutional dopants alter the electronic structure and the photon absorption efficiency of TiO₂ and induce an electronic coupling effect with the TiO₂ atoms.⁵⁸ After hydrogen doping, the bandgap reached a value of 2.80 eV and 2.85 eV for H_i [Figs. 9(b) and 10(b)] and H_O [Figs. 9(c) and 10(c)], respectively. In both cases, mid-gap states are created. Those states are favorable paths for electron transport, hence improving the electron transport capability of the oxide while the bandgap reduction increases its light absorption efficiency.

Finally, for the Sn_{Ti}:TiO₂ (Figs. 11 and 12) case, we predicted that the bandgap is calculated as 3 eV. Mehraz *et al.*⁶⁰ performed experiments and concluded that with a 1% Sn doping, the bandgap is reduced 0.2 eV, which is similar to the reduction we predicted. When hydrogen is in the interstitial position, the bandgap reaches a value of 2.75 eV and mid-gap states are created at 1.95 eV. However, when H is substitutional of O, the bandgap reaches a value of 2.88 eV with gap states at 1.80 eV.

From all the above, it is expected that when TiO₂ is doped with carbon family elements, the bandgap is reduced with the most prominent reduction occurring with the Si_{Ti} case. When hydrogen is inserted in the interstitial position, then the bandgap has the lowest value (2.75 eV) in the case of H_i:Sn_{Ti}:TiO₂. On the other hand, when hydrogen is inserted as a substitutional defect, the lowest bandgap is 2.70 eV for H_O:Si_{Ti}:TiO₂. This value is one of the lowest bandgap values predicted for the doped TiO₂. For example, in the case of the halogen doped TiO₂, we had predicted in a

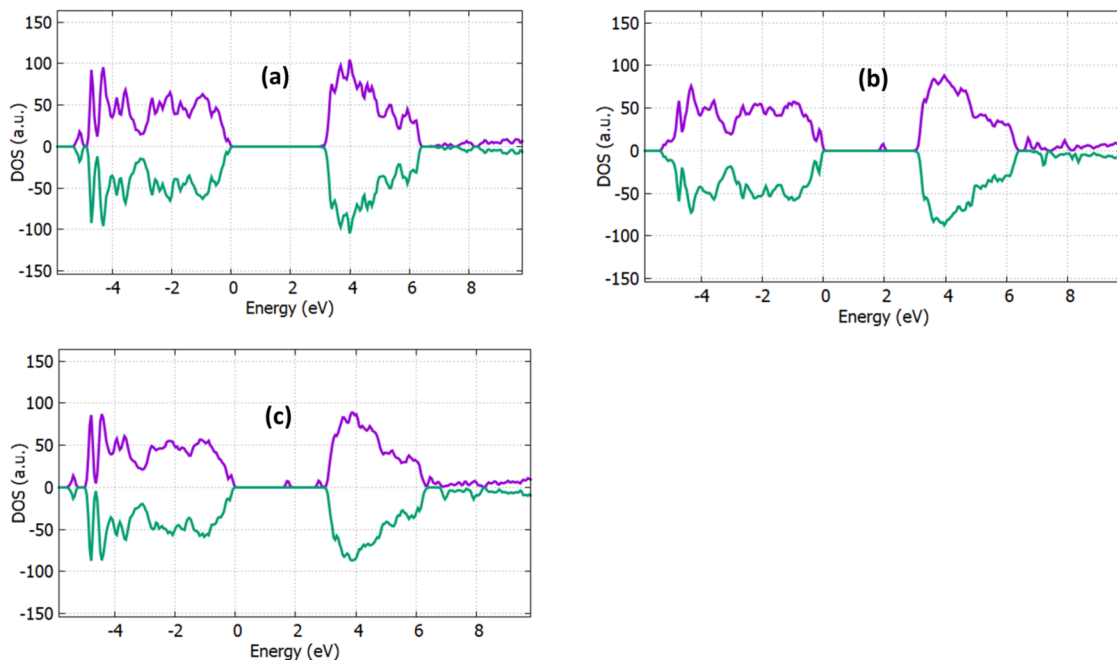


FIG. 7. Densities of states for (a) Si_{Ti}, (b) H_i and Si_{Ti}, and (c) H_O and Si_{Ti} doped TiO₂.

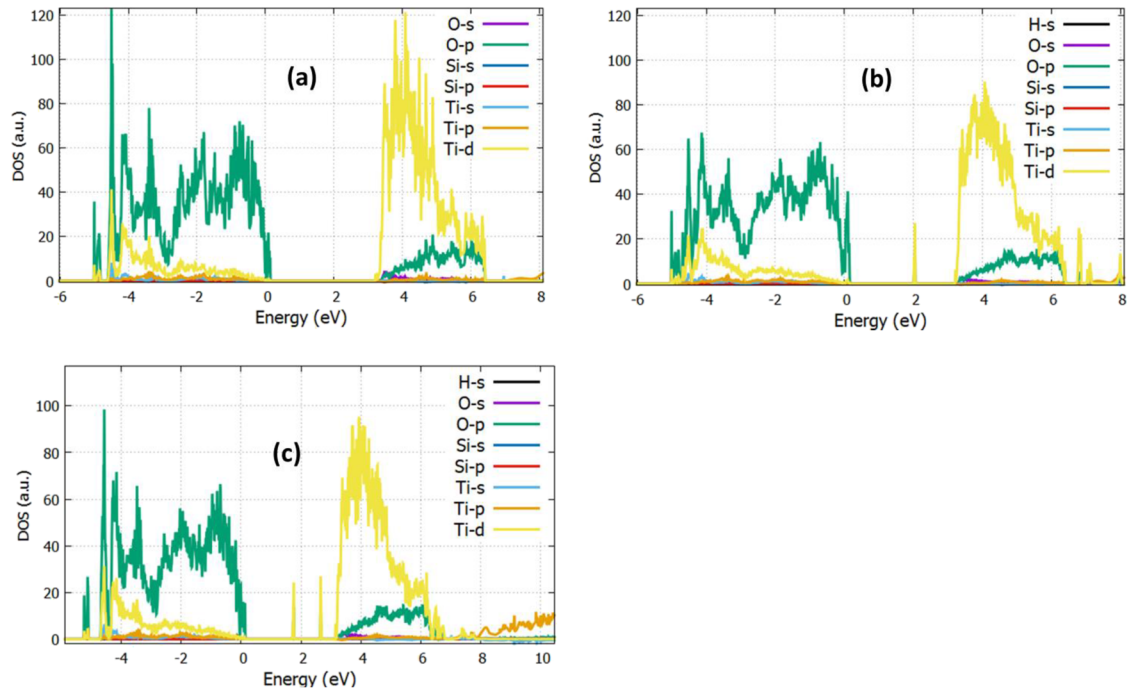


FIG. 8. Projected densities of states for (a) Si_{Ti} , (b) H_i and Si_{Ti} , and (c) H_O and Si_{Ti} doped TiO_2 .

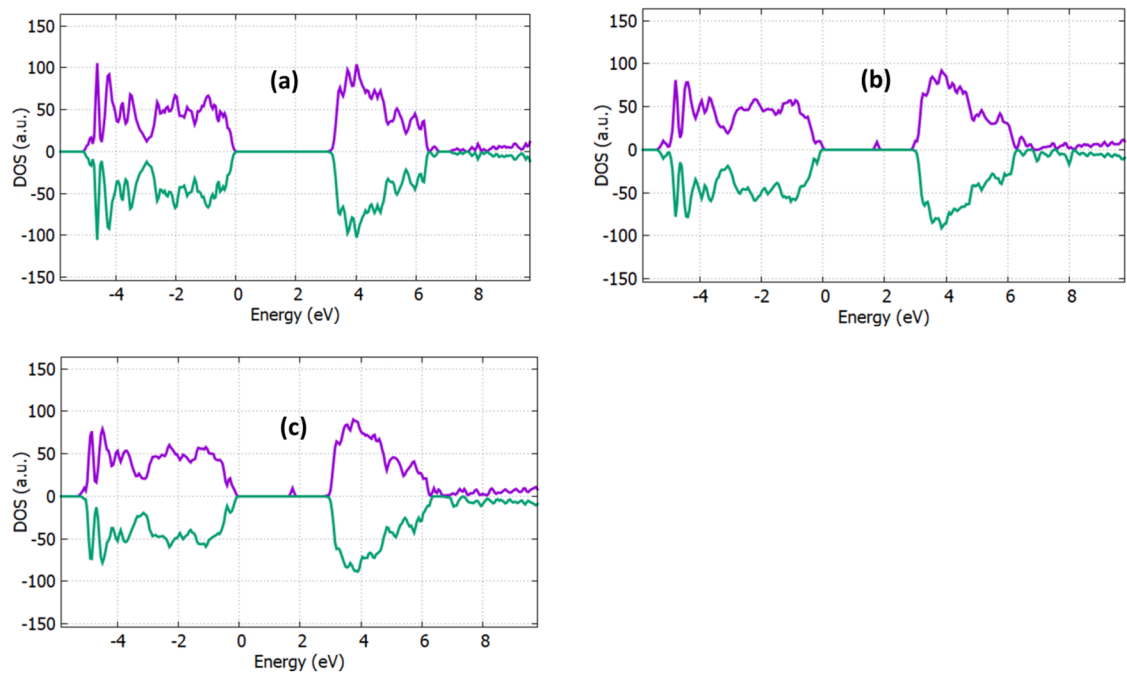


FIG. 9. Densities of states for (a) Ge_{Ti} , (b) H_i and Ge_{Ti} , and (c) H_O and Ge_{Ti} doped TiO_2 .

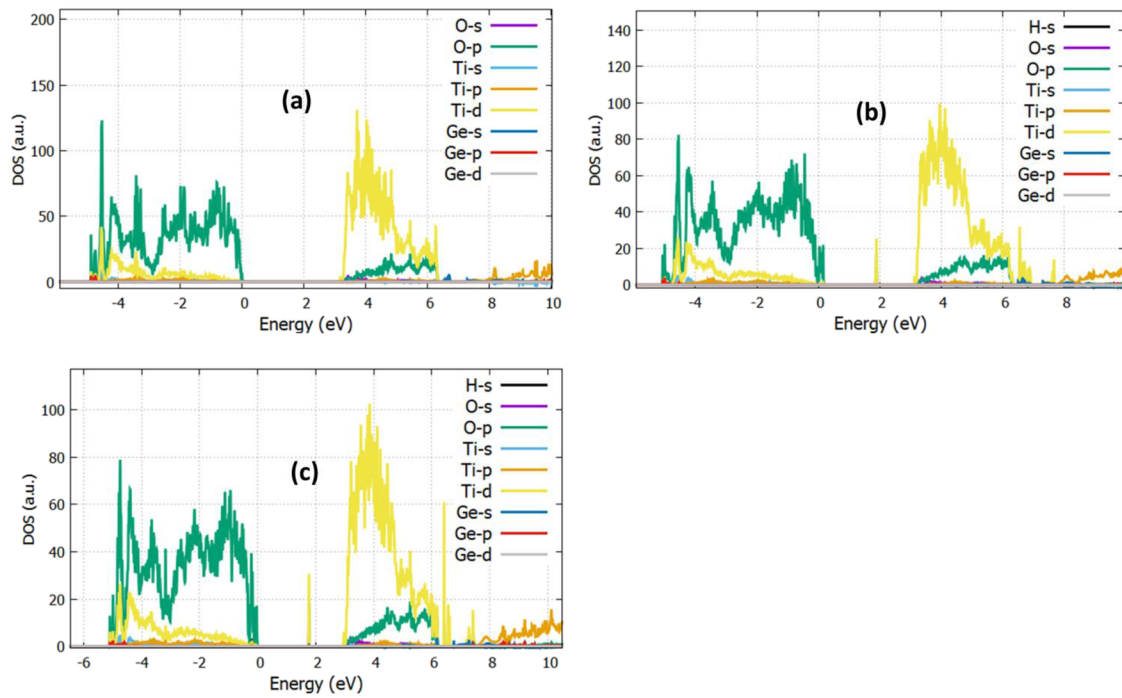


FIG. 10. Projected densities of states for (a) GeTi , (b) Hf , and (c) Hf and GeTi doped TiO_2 .

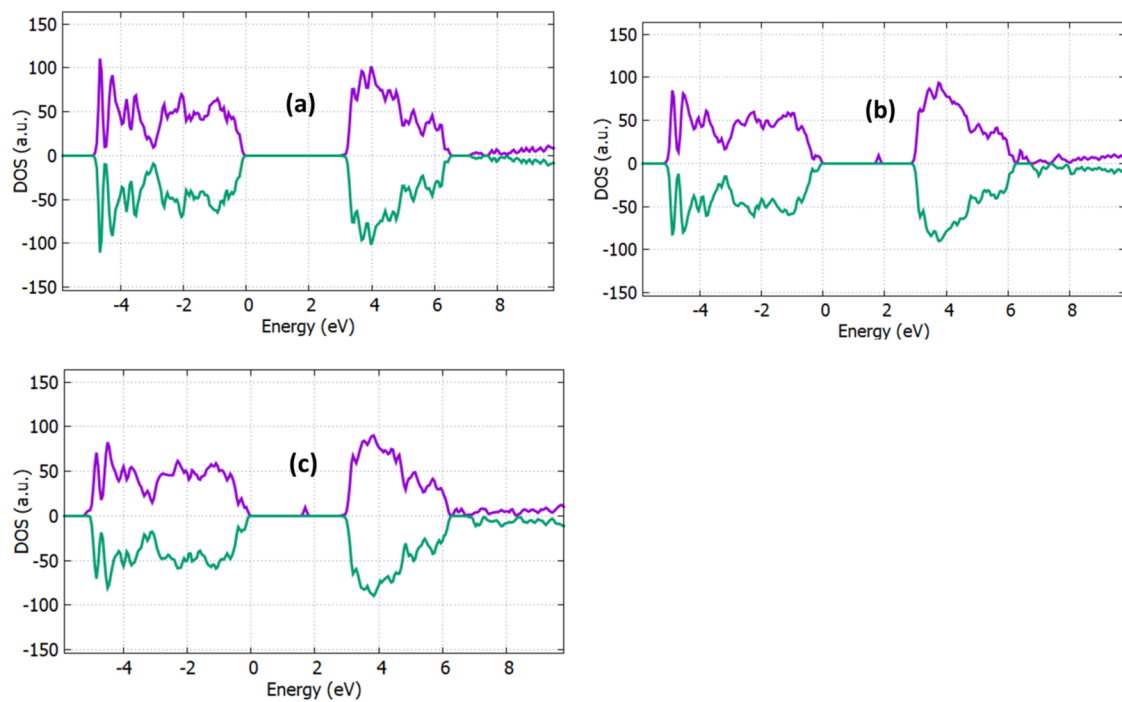


FIG. 11. Densities of states for (a) SnTi , (b) Hf , and (c) Hf and SnTi doped TiO_2 .

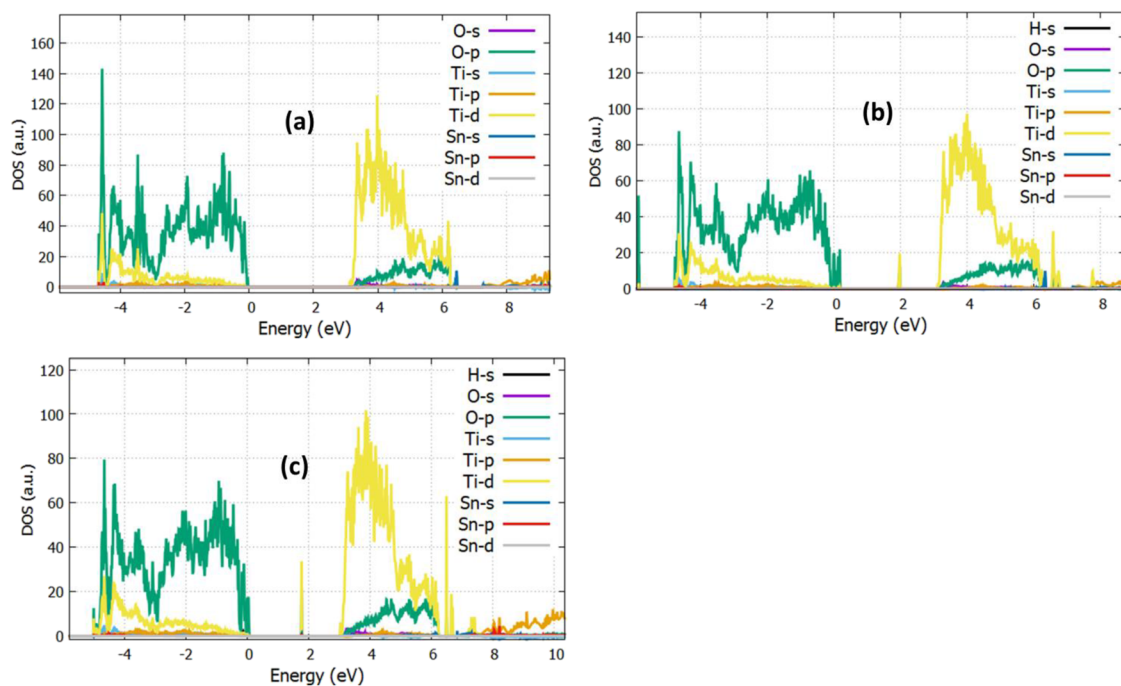


FIG. 12. Projected densities of states for (a) SnTi , (b) H , and (c) H_2O and SnTi doped TiO_2 .

previous work that the lowest bandgap value (2.9 eV) is achieved with $\text{Cl}:\text{TiO}_2$.¹⁴ A significant reduction of the bandgap (2.43 eV) was achieved with $\text{Cr}:\text{TiO}_2$; however, it was under a constant pressure environment.¹⁵

IV. CONCLUSIONS

In the present study, we performed calculations on the structural and electronic properties of TiO_2 in the cases of doping with $\text{X}(\text{C, Si, Ge, Sn})$ and co-doping with X and H . It is revealed that Si doping can significantly reduce the lattice parameters and the volume of the supercell. It is seen that in all the cases, hydrogen incorporation in interstitial and substitutional sites does not significantly alter the lattice parameters. To reveal the advantages of hydrogen co-doping on the Si-doped TiO_2 , we performed DOS calculations and predicted that the most prominent bandgap reduction occurs when hydrogen sites to the oxygen position. Taking into account that in experiments there are many oxygen vacancies, it is expected that hydrogen is more favorable to occupy an oxygen position. Here, we show that hydrogenation has a positive impact on the structural and electronic properties of TiO_2 , thus making it an appropriate candidate for energy harvesting devices. We conclude that it is imperative to experimentally examine $\text{H}:\text{Si}:\text{TiO}_2$, as the bandgap reduction could be beneficial for energy device applications.

ACKNOWLEDGMENTS

The authors declare that there is no competing financial interest.

DATA AVAILABILITY

The data that support the findings of this study are available from the corresponding author upon reasonable request.

REFERENCES

- A. Fujishima and K. Honda, *Nature* **238**(5358), 37 (1972).
- M. Grätzel, *Nature* **414**, 338 (2001).
- R. Asahi, T. Morikawa, T. Ohwaki, K. Aoki, and Y. Taga, *Science* **293**, 269 (2001).
- S. U. M. Khan, M. Al-Shahry, and W. B. Ingler, *Science* **297**, 2243 (2002).
- S. P. Russo, I. E. Grey, and N. C. Wilson, *J. Phys. Chem. C* **112**, 7653 (2008).
- H. G. Yang, C. H. Sun, S. Z. Qiao, J. Zou, G. Liu, S. C. Smith, H. M. Cheng, and G. Q. Lu, *Nature* **453**, 638 (2008).
- Y. Gai, J. Li, S.-S. Li, J.-B. Xia, and S.-H. Wei, *Phys. Rev. Lett.* **102**, 036402 (2009).
- M. Vasilopoulou, D. G. Georgiadou, A. Soultati, N. Boukos, S. Gardelis, L. C. Palilis, M. Fakis, G. Skoulatakis, S. Kennou, M. Botzakaki, S. Georga, C. A. Krontiras, F. Auras, D. Fattakhova-Rohlfing, T. Bein, T. A. Papadopoulos, D. Davazoglou, and P. Argitis, *Adv. Energy Mater.* **4**, 1400214 (2014).
- K. Sivula and R. van de Krol, *Nat. Mater. Rev.* **1**, 15010 (2016).
- J. Zhu, M. Vasilopoulou, D. Davazoglou, S. Kennou, A. Chroneos, and U. Schwingenschlög, *Sci. Rep.* **7**, 40882 (2017).
- B. Santara, P. K. Giri, K. Imakita, and M. Fujii, *J. Phys. Chem. C* **117**, 23402 (2013).
- X. Gao and I. E. Wachs, *Catal. Today* **51**, 233 (1999).
- N. Seriani, C. Pinilla, S. Cereda, A. De Vita, and S. Scandolo, *J. Phys. Chem. C* **116**, 11062 (2012).
- P. P. Filippatos, N. Kelaidis, M. Vasilopoulou, D. Davazoglou, N. N. Lathiotakis, and A. Chroneos, *Sci. Rep.* **9**, 19970 (2019).
- N. Kelaidis, A. Kordatos, S.-R. G. Christopoulos, and A. Chroneos, *Sci. Rep.* **8**, 12790 (2018).
- X. Chen, L. Liu, P. Y. Yu, and S. S. Mao, *Science* **331**, 746–750 (2011).

- ¹⁷L. Liu, P. Y. Yu, X. Chen, S. S. Mao, and D. Z. Shen, *Phys. Rev. Lett.* **111**, 065505 (2013).
- ¹⁸M. Vasilopoulou, N. Kelaidis, E. Polydorou, A. Soultati, D. Davazoglou, P. Argitis, G. Papadimitropoulos, D. Tsikritzis, S. Kennou, F. Auras, D. G. Georgiadou, S.-R. G. Christopoulos, and A. Chroneos, *Sci. Rep.* **7**, 17839 (2017).
- ¹⁹S. Islam, S. Nagpure, D. Kim, and S. Rankin, *Inorganics* **5**, 15 (2017).
- ²⁰C. Salazar-Ballesteros, "Kinetic Studies on the role of hydrogen-bonding interactions in the TiO₂ photooxidation of small polar organic compounds in aqueous solution," Ph.D. thesis, University of Oklahoma, USA, 2009.
- ²¹C. Yang, Z. Wang, T. Lin, H. Yin, X. Lü, D. Wan, T. Xu, C. Zheng, J. Lin, F. Huang, X. Xie, and M. Jiang, *J. Am. Chem. Soc.* **135**, 17831 (2013).
- ²²W. Choi, A. Termin, and M. R. Hoffmann, *J. Phys. Chem.* **98**, 13669 (1994).
- ²³K. E. Karakitsou and X. E. Verykios, *J. Phys. Chem.* **97**, 1184 (1993).
- ²⁴H. Yamashita, Y. Ichihashi, M. Takeuchi, S. Kishiguchi, and M. Anpo, *J. Synchrotron Radiat.* **6**, 451 (1999).
- ²⁵M. Anpo, *Green Chemistry* (Oxford University Press, Oxford, 2000).
- ²⁶S. Sakthivel and H. Kisch, *Angew. Chem., Int. Ed.* **42**, 4908 (2003).
- ²⁷G. Wu, T. Nishikawa, B. Ohtani, and A. Chen, *Chem. Mater.* **19**, 4530 (2007).
- ²⁸H. Irie, Y. Watanabe, and K. Hashimoto, *Chem. Lett.* **32**, 772 (2003).
- ²⁹K. Noworyta and J. Augustynski, *Electrochem. Solid State Lett.* **7**, E31 (2004).
- ³⁰H. Gao, C. Ding, and D. Dai, *J. Mol. Struct.: THEOCHEM* **944**, 156 (2010).
- ³¹L. Xu, C.-Q. Tang, and J. Qian WuliXuebao, *Acta Phys. Sin.* **59**, 2721 (2010).
- ³²J. Yu, G. Dai, Q. Xiang, and M. Jaroniec, *J. Mater. Chem.* **21**, 1049 (2011).
- ³³J. Yu, P. Zhou, and Q. Li, *Phys. Chem. Chem. Phys.* **15**, 12040 (2013).
- ³⁴Z. Li, W. Xia, and L. Jia, *Can. J. Phys.* **92**, 71 (2014).
- ³⁵S.-M. Oh, S.-S. Kim, J. E. Lee, T. Ishigaki, and D.-W. Park, *Thin Solid Films* **435**, 252 (2003).
- ³⁶X. Yan, J. He, D. G. Evans, X. Duan, and Y. Zhu, *Appl. Catal., B* **55**, 243 (2005).
- ³⁷H. Ozaki, S. Iwamoto, and M. Inoue, *Chem. Lett.* **34**, 1082 (2005).
- ³⁸R. Long, Y. Dai, G. Meng, and B. Huang, *Phys. Chem. Chem. Phys.* **11**, 8165 (2009).
- ³⁹J. Li and H. C. Zeng, *J. Am. Chem. Soc.* **129**, 15839 (2007).
- ⁴⁰C. Xiong, Jr. and K. J. Balkus, *J. Phys. Chem. C* **111**, 10359 (2007).
- ⁴¹M. C. Payne, M. P. Teter, D. C. Allan, T. A. Arias, and J. D. Joannopoulos, *Rev. Mod. Phys.* **64**, 1045 (1992).
- ⁴²M. D. Segall, P. J. D. Lindan, M. J. Probert, C. J. Pickard, P. J. Hasnip, S. J. Clark, and M. C. Payne, *J. Phys.: Condens. Matter* **14**, 2717 (2002).
- ⁴³J. P. Perdew, K. Burke, and M. Ernzerhof, *Phys. Rev. Lett.* **77**, 3865 (1996).
- ⁴⁴D. Vanderbilt, *Phys. Rev. B* **41**, 7892 (1990).
- ⁴⁵H. J. Monkhorst and J. D. Pack, *Phys. Rev. B* **13**, 5188 (1976).
- ⁴⁶E. M. Kiarii, K. K. Govender, P. G. Ndungu, and P. P. Govender, *Chem. Phys. Lett.* **678**, 167 (2017).
- ⁴⁷A. Kordatos, N. Kelaidis, and A. Chroneos, *Solid State Ionics* **315**, 40–43 (2018).
- ⁴⁸A. Kordatos, N. Kelaidis, and A. Chroneos, *J. Appl. Phys.* **123**, 161510 (2018).
- ⁴⁹D. O. Scanlon, C. W. Dunnill, J. Buckeridge, S. A. Shevlin, A. J. Logsdail, S. M. Woodley, C. R. A. Catlow, M. J. Powell, R. G. Palgrave, I. P. Parkin, G. W. Watson, T. W. Keal, P. Sherwood, A. Walsh, and A. A. Sokol, *Nat. Mater.* **12**, 798–801 (2013).
- ⁵⁰F. De Angelis, C. Di Valentin, S. Fantacci, A. Vittadini, and A. Selloni, *Chem. Rev.* **114**, 9708–9753 (2014).
- ⁵¹H. Wang, A. Chroneos, C. A. Londos, E. N. Sgourou, and U. Schwingenschlögl, *Sci. Rep.* **4**, 4909 (2014).
- ⁵²A. Chroneos, E. N. Sgourou, C. A. Londos, and U. Schwingenschlögl, *Appl. Phys. Rev.* **2**, 021306 (2015).
- ⁵³J. Muscat, V. Swamy, and N. W. Harrison, *Phys. Rev. B* **65**, 224112 (2002).
- ⁵⁴D. Chen, Z. Jiang, J. Geng, Q. Wang, and D. Yang, *Ind. Eng. Chem. Res.* **46**, 2741–2746 (2007).
- ⁵⁵N. Li, K. L. Yao, L. Li, Z. Y. Sun, G. Y. Gao, and L. Zhu, *J. Appl. Phys.* **110**, 073513 (2011).
- ⁵⁶Y. Su, S. Chen, X. Quan, H. Zhao, and Y. Zhang, *Appl. Surf. Sci.* **255**, 2167 (2008).
- ⁵⁷W. Shi, Q. Chen, Y. Xu, D. Wu, and C.-f. Huo, *J. Solid State Chem.* **184**(8), 1983 (2011).
- ⁵⁸S. Chatterjee and A. Chatterjee, *Jpn. J. Appl. Phys., Part 1* **47**, 1136 (2008).
- ⁵⁹Y. Duan, N. Fu, Q. Liu, Y. Fang, X. Zhou, J. Zhang, and Y. Lin, *J. Phys. Chem. C* **116**, 8888 (2012).
- ⁶⁰S. Mehrzad, P. Kongsong, A. Taleb, N. Dokhane, and L. Sikong, *Sol. Energy Mater. Sol. Cells* **189**, 254 (2019).
- ⁶¹Y. Lin, Z. Jiang, X. Hu, X. Zhang, and J. Fan, *Appl. Phys. Lett.* **100**, 102105 (2012).
- ⁶²J. Chang, Z.-Y. Jiang, Z.-Y. Zhang, Y.-M. Lin, P.-L. Tian, B. Zhou, and L. Chen, *Appl. Surf. Sci.* **484**, 1304 (2019).